Solar Energy 142 (2017) 97–108

Contents lists available at ScienceDirect

Solar Energy

journal homepage: www.elsevier.com/locate/solener

Prototype fabrication and experimental investigation of a conjugate refractive reflective homogeniser in a cassegrain concentrator

Katie Shanks [a,*], Hasan Baig [a], N. Premjit Singh [b], S. Senthilarasu [a], K.S. Reddy [b], Tapas K. Mallick [a,*]

[a] Environment and Sustainability Institute, University of Exeter, Penryn Campus, Penryn TR10 9FE, UK
[b] Heat Transfer and Thermal Power Laboratory, Department of Mechanical Engineering, Indian Institute of Technology Madras, Chennai 600 036, India

ARTICLE INFO

Article history:
Received 1 September 2016
Received in revised form 21 November 2016
Accepted 22 November 2016
Available online 22 December 2016

Keywords:
Concentrator photovoltaics
Cassegrain
Optical loss
Materials
Temperature
Homogeniser

ABSTRACT

The conjugate refractive reflective homogeniser (CRRH) is experimentally tested within a cassegrain concentrator of geometrical concentration ratio 500× and its power output compared to the theoretical predictions of a 7.76% increase. I–V traces are taken at various angles of incidence and experimental results showed a maximum of 4.5% increase in power output using the CRRH instead of its purely refractive counterpart. The CRRH utilises both total internal reflection (TIR) within its core refractive medium (sylguard) and an outer reflective film (with an air gap between) to direct more rays towards the receiver. The reflective film captures scattered refracted light which is caused by non-ideal surface finishes of the refractive medium. The CRRH prototype utilises a 3D printed support which is thermally tested, withstanding temperatures of up to 60 °C but deforming at >100 °C. A maximum temperature of 226.3 °C was reached within the closed system at the focal spot of the concentrated light. The material properties are presented, in particular the transmittance of sylguard 184 is shown to be dependent on thickness but not significantly on temperature.

Utilising both TIR and standard reflection can be applied to other geometries other than the homogeniser presented here. This could be a simple but effective method to increase the power of many concentrator photovoltaics.

1. Introduction

Concentrator photovoltaic (CPV) designs have been pushing higher concentration ratios to achieve higher conversion efficiencies and cost effectiveness. As the concentration ratio of an optic is increased, the acceptance-angle decreases, making it more difficult to manage the design deviations and uncertainties (optical tolerances) (Baig et al., 2012; Canavarro et al., 2013). A homogeniser optic is typically needed to match beam shape and size to the receiver and improve the optical tolerance of the overall optical system (Baig et al., 2012; Canavarro et al., 2013). Final stage optics within a CPV commonly take the form of a compound Parabolic Concentrator or V-trough but other shapes are being investigated such as the dome lens (Hatwaambo et al., 2008; Shanks et al., 2016c, 2015; Victoria et al., 2009; Winston, 1970). There are homogenising optical designs with varying advantages already available but as designs progress and perhaps become more complex the material, surface quality and solar cell coupling method needs to be further investigated.

One key consideration in all of the above named designs is the material to be used and the resulting surface quality (Fend et al., 2003; Yin and Huang, 2008). Previous simulation work has been carried out to show the importance of considering the surfaced roughness and subsequent light scattering during the design and simulation stages of development (Shanks et al., 2016a). This previous study investigated a cassegrain concentrator design similar to that of SolFocus (Gordon et al., 2008) but focused on the surface quality of the refractive homogenising optic. The system presented here and in the previous work was optimised for acceptance angle (Shanks et al., 2016b). There are many cassegrain concentrators which have been investigated in the past (Chen and Ho, 2013; Chong et al., 2013; Dreger et al., 2014; McDonald et al., 2007; Roman et al., 1995; Terry et al., 2012, 1996; Victoria et al., 2013; Yehezkel et al., 1993) but further insight into the material and manufacturing choices is needed. Cassegrain set ups are known for having slightly lower acceptance angles than their Fresnel lens counterparts but can reach higher concentration ratios and hence why this type of system was chosen to not only understand the

* Corresponding authors.
E-mail addresses: kmas201@exeter.ac.uk (K. Shanks), H.Baig@exeter.ac.uk (H. Baig), premjitmtech@gmail.com (N.P. Singh), S.Sundaram@exeter.ac.uk (S. Senthilarasu), ksreddy@iitm.ac.in (K.S. Reddy), T.K.Mallick@exeter.ac.uk (T.K. Mallick).

http://dx.doi.org/10.1016/j.solener.2016.11.038
0038-092X/

design constraints but see if a new homogeniser would improve the performance, especially for future designs of higher solar concentration levels. The surface roughness of refractive optics which utilise total internal reflection (most homogenisers) causes scattering of incoming light and incomplete TIR despite incident light fulfilling the acceptance angle criteria of the optic. Surface imperfections will also increase the reflection upon entering the refractive optic. The degree of this surface inhomogeneity depends on the manufacturing process and material used with higher quality optical finishes and coatings costing more (Yin and Huang, 2008).

As indicated in the previous theoretical study (Shanks et al., 2016a), high quality glass homogenisers and similar refractive optics which utilise TIR will not suffer much optical loss due to poor surface quality. Glass is the preferred choice of material to achieve very smooth and accurate optical finishes and the inverted pyramid glass homogeniser and CPC optics can be bought off the shelf at reasonable costs. However, more complex prototypes are costly to fabricate using glass and even if glass is used these optics then need to be attached optically to the solar cells using an encapsulate. When coupling a homogeniser to a solar cell as a secondary step, the lateral spillage of the silicone causes significant optical losses from leakage through it. If to avoid spillage the joint is under-filled, the joint could be weaker and possibly result in an air gap also producing optical losses (Benítez et al., 2010). These losses cannot be quantified until full production is achieved. In the present study we have eliminated the step of the optical coupling the solar cell separately with the solar cell by preparing a mould, which allows this.

In this way we can manufacture the V-trough homogeniser, simultaneously join it to the solar cell and reduce alignment errors by using this mould. To do this we use the refractive material Sylguard 184 which is predominantly used as an encapsulate and has the advantage of setting at room temperature. This is important as we should not subject the cell to any unnecessary heating before use and because typical high temperature mould setting can involve expansion and contraction of the material which could damage the solar cell when part of a closed mould such as this.

As already discussed, using an alternative material to glass will most likely result in more surface scattering. To compensate for this we add an outer reflective casing with an air gap to ensure both TIR and standard reflection can occur, trapping scattered rays. This hence becomes the Conjugate Refractive Reflective Homogeniser (CRRH).

Identifying the losses within a homogenizer of a high concentrating photovoltaic system, quantifying them and applying simple solutions towards improving them will improve the performance of the full system. Within the growing area of solar concentrator research there needs to be a clearer understanding of how theoretical designs will perform in real conditions with real optics. For this reason this paper is the experimental counterpart to a previous theoretical study on the CRRH within a cassegrain concentrator (Shanks et al., 2016a). Hence, one of the focuses of this study is to confirm how much of the theoretical predictions could be realised (7.76% theoretical power increase), what materials and manufacturing methods are feasible and their performance in a high temperature environment.

At present, manufacturing processes for optics include precise grinding, milling, polishing, and a variety of coating methods for a smooth finish (Xu et al., 2013). Most current manufacturing processes struggle to produce acceptable priced prototype optics of new specific shapes and reliable accuracy (Kaushika and Reddy, 2000; Tsai, 2013). Here, we have tested plastic mirrors for their advantages in cost, weight and smooth surface quality. One of the challenges of CPV technology is its increased initial investment in comparison to flat plate PV due to the added optics and tracking required (Fraas, 2014). Computer-controlled diamond turning machines, as well as other modern materials and moulding techniques, have significantly improved the design and accuracy of refractive optics such as Fresnel lenses (Leutz and Suzuki, 2001). In this study we have utilised 3D printing and tested a structure for its heat tolerance within a CPV system. 3D printing is a very powerful prototyping tool which needs further testing for use within CPV research. The 3D printed support structure also compensates for the possibly weaker coupling joint of the 1 step moulding. This study, though specific in design and material, highlights a general issue in optics and prototyping and suggests simple but effective methods of compensating for losses due to surface roughness.

2. Theoretical work

A previous study has been undertaken which optimised a cassegrain concentrator design of 500× geometrical concentration (Shanks et al., 2016b). This design was optimised for acceptance angle by investigating the ray displacement at 1° incidence angle for a range of focal length and separation distance parameter of the two reflector dishes in the system. Use of a homogeniser was required to improve the acceptance angle of the cassegrain set up and a refractive homogeniser was chosen instead of a reflective one to take advantage of total internal reflection (TIR). As already discussed this TIR is however only fully effective if the homogeniser surface quality is very smooth. In the previous study, this tall homogeniser optic was found to lean when the system was tilted to track the sun (Shanks et al., 2016b). For all these reasons a new homogeniser optic utilising an outer reflective casing was proposed and investigated also (Shanks et al., 2016a). This previous study focused on the theoretical concept of compensating for surface roughness in the homogeniser by catching refracted rays with a reflective film. Various materials and surface structures were investigated (Shanks et al., 2016a). Manufacturing the optic however needed to be done in a reliable and effective manner. Hence, the reports here utilising 3D printing.

The cassegrain concentrator and its final dimensions can be seen in Fig. 1 (Shanks et al., 2016b). The design aimed to simultaneously obtain a high optical efficiency and a good acceptance angle. The concentrator consisted of a parabolic primary reflector, inverse parabolic secondary reflector and a refractive crossed V-trough homogenising tertiary as shown in Fig. 1. In comparison to the SolFocus design (Gordon et al., 2008), the primary parabolic dish has a higher focal length (270 mm) and a taller homogeniser (75 mm). Everything has also been cut to a square shape to allow compact arrays. Manufacturing uncertainties were considered and various material surface scattering profiles of the optics in the system were simulated (Shanks et al., 2016a). A 3–42% drop in optical efficiency was shown to occur (Fig. 2) depending on the material and scattering profile of the homogeniser.

Hence, the new conjugate refractive-reflective homogeniser (CRRH) was proposed as a solution to improve the homogeniser optical losses. The CRRH utilises the addition of a straight reflective film to the dielectric homogeniser with a 1 mm air gap kept between the dielectric medium and reflective film. The reflective sleeve ensures total internal reflection is maintained for the majority of light rays and the previously lost scattered light is also caught. This simple but effective method to recover rays which fail TIR has been used elsewhere (Baig, 2015). Baig et al. (2015, 2014) discuss the optical losses caused by the encapsulation medium used in connecting low concentration optics to solar cells. Light rays incident in this overlap region do not reflect towards the solar cell but continue through the encapsulation medium until lost.

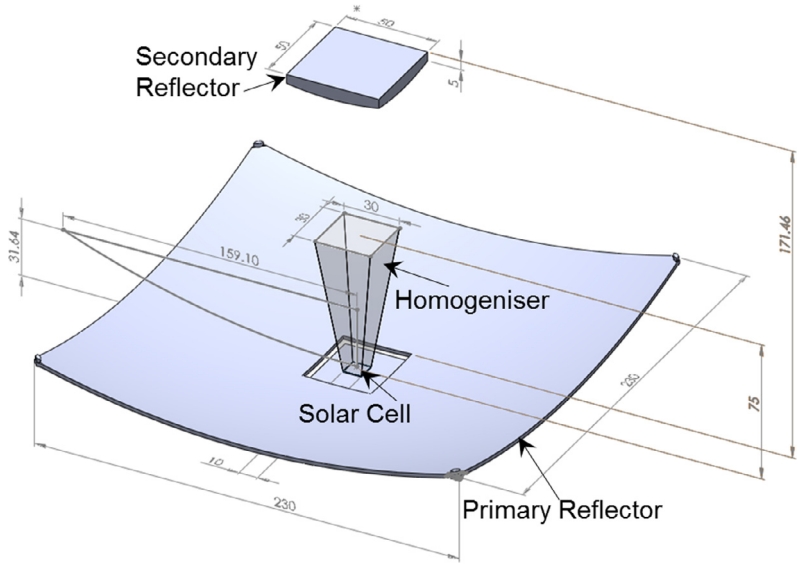

Fig. 1. Cassegrain design with large primary parabolic reflector and secondary parabolic reflector with dimensions in mm. The primary paraboloid has a focal length of 270 mm and the secondary paraboloid a focal length of 70 mm. Both parabolic reflectors are afocal in relation to each other and cut to square shapes for compact array placement.

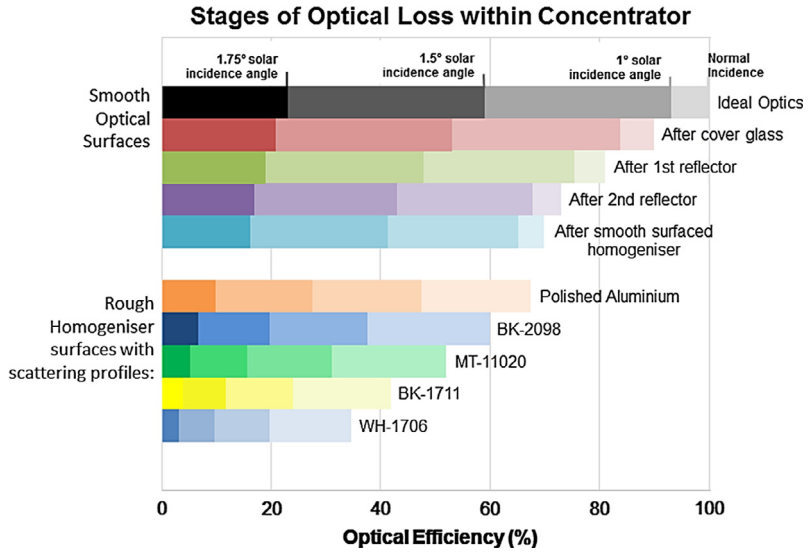

Fig. 2. Theoretical contribution of optical losses from different optical stages/surfaces calculated from ray trace simulations (Shanks et al., 2016a).

Baig et al. overcame the encapsulation issue by adding a strip of reflective film to the bottom edge of the 3D cross compound parabolic concentrator designed for building integration (Baig et al., 2015, 2014). We have expanded on this method by applying reflective film with a 1 mm air gap to all of the TIR active walls of a homogeniser in a high concentration cassegrain concentrator.

The effects of the air gap size and reflective film angle and material was investigated in the previous study (Shanks et al., 2016a). Ultimately, the findings confirmed that the addition of the reflective film did improve the optical efficiency of the optic but its angle and the size of the air gap made little difference. As small air gap as possible is optimum but an air gap is essential to ensure TIR still takes place or there is a significant reduction in optical loss due to multiple standard reflections. Other shapes such as an outer compound parabolic concentrator reflective film could also be investigated. Although the optical efficiency may not improve much by using a CPC shaped reflective casing, the acceptance angle may benefit. A reliable method of manufacturing would still be necessary to ensure the added complexity of a CPC CRRH did not result in excessive cost. The flat reflective film sleeve was chosen in this study due to its simplicity and low cost especially for the prototyping stage of a concentrator. Once proven and manufactured effectively with the best materials, more complex curves can be investigated more effectively.

We have also eliminated the homogeniser to solar cell coupling stage and minimised the encapsulate spillage by moulding everything together at once using the same refractive material. Hence, the conjugate refractive reflective homogeniser (CRRH) as shown in Fig. 3.

In the theoretical study carried out previously (Shanks et al., 2016a), the CRRH (Fig. 3a) increased the overall optical efficiency by a maximum of 7.75% in comparison to that of a standard refractive homogeniser (Fig. 3b) simulated within the same concentrator system. This value depended on the material used and surface

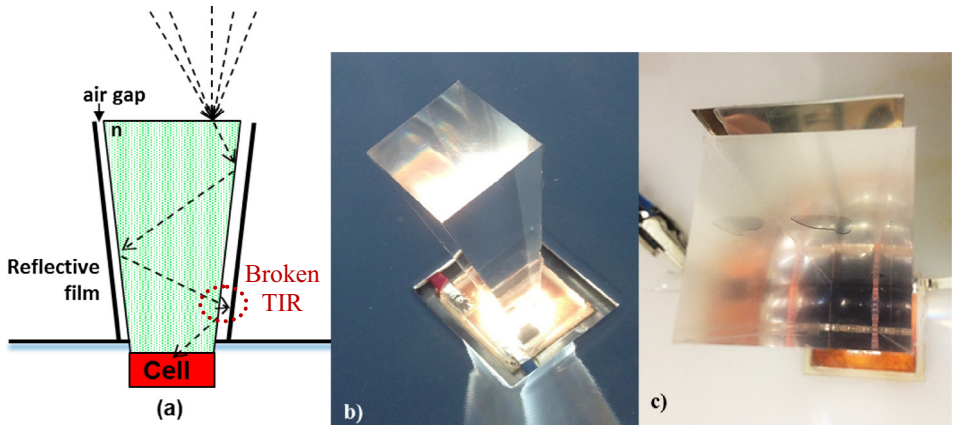

Fig. 3. (a) Diagram of the conjugate refractive reflective homogeniser showing a light ray which eventually does not undergo TIR but is still reflected by the layer of reflective film. (b) Photo of refractive homogeniser attached to 10 mm × 10 mm multijunction solar cell. (c) Photo of refractive homogeniser with reflective film sleeve on one side (making the CRRH) for initial validation results given in (Shanks et al., 2016a). The effect of no air gap (where the reflective film is sticking to the refractive medium half way down the side) which voids TIR and causes non ideal standard reflection can also be seen.

roughness of the refractive part of the homogenisers in use (Shanks et al., 2016a). The CRRH (Fig. 3c) was also validated via practical measurements and a 6.7% power increase was measured under a 1000 W/m^2 solar simulator at normal incidence for the experimental test (Shanks et al., 2016a). This test however used a Fresnel lens set up of a different focal length and wavelength dispersion than that of the simulated cassegrain concentrator. Although the result still validates the benefit of the CRRH, further experimental investigation is required to compare the theoretical to the experimental, especially for varying incidence angle. The reliability of the materials must also be tested experimentally. As mentioned earlier the acceptance angle becomes increasingly important as the concentration ratio increases. Fig. 4b illustrates the different losses within the cassegrain system when the module is misaligned with the sun. The red numbered circles in Fig. 4b highlight the main areas of loss which are otherwise optimised as shown by the lettered red circles in Fig. 4a. These lost rays in Fig. 4b are responsible for the reduced optical efficiency in Fig. 2 at increased solar incidence angles when the optical materials are simulated as ideal but the geometry still loses light.

The CRRH minimises the optical losses at site no. 4 in Fig. 4b but other areas of loss are inevitable with increased solar incidence angle due to the acceptance angle limitations of the design.

High and ultrahigh concentrator designs rely heavily on high accuracy which often leads to high expense. Here, we compare the experimental performance of the CRRH within a 500× cassegrain concentrator to the same system with a standard refractive homogeniser (Fig. 3b). Measurements are taken over a range of solar misalignment angles to show the effect on acceptance angle for this type of system. The experimental results obtained are also compared to the theoretical predictions in the previous study to show how much of the theoretical gain with the CRRH is actually realistically achievable – an important factor sometimes overlooked in theoretical design proposals.

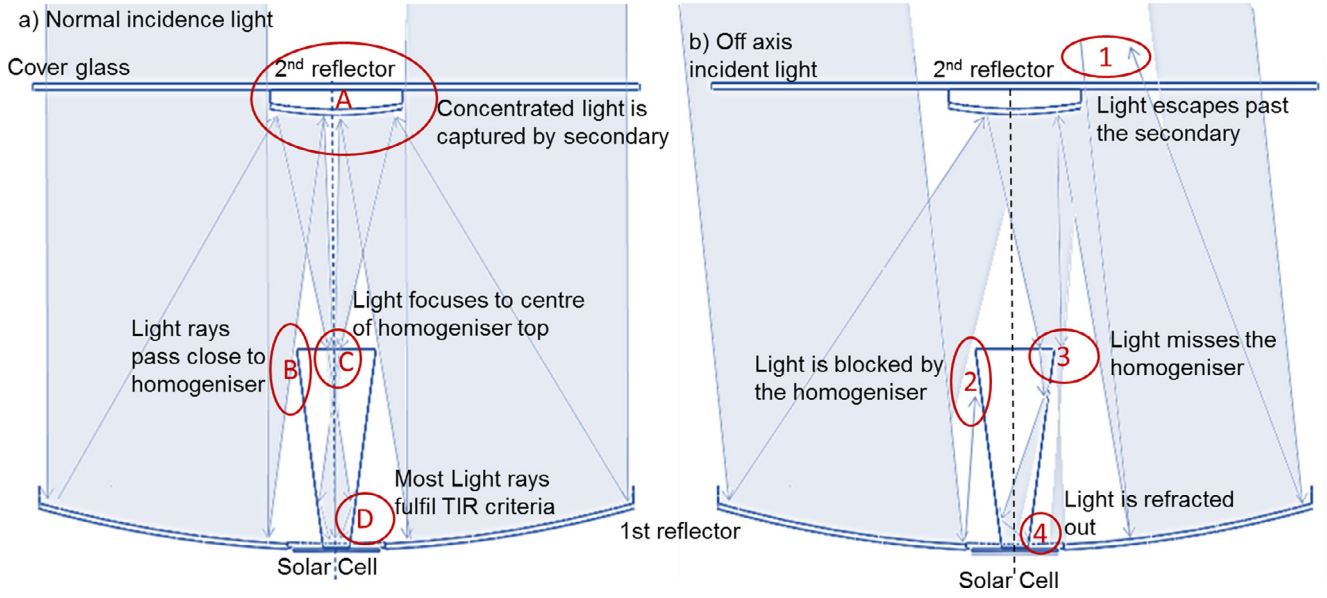

Fig. 4. (a) Diagram of light ray propagation through the cassegrain concentrator when incoming light is normal to the system and components are aligned perfectly towards the sun. Key design features at normal incidence are highlighted with lettered red circles. (b) Diagram of lost light rays due to misalignment with sun. Areas of loss are highlighted with numbered red circles. (For interpretation of the references to color in this figure legend, the reader is referred to the web version of this article.)

3. Materials and manufacturing

Prototypes are difficult to manufacture cost effectively. As mentioned earlier there is always at least some loss with each additional optical stage and component material interface introduced (Fig. 2). Unless very accurate and also expensive manufacturing procedures are employed, these losses increase in the prototyping stage. 90% efficient primary and secondary reflectors in particular were difficult to obtain for this prototype. The low iron glass cover was measured as being ~90% transparent (Fig. 5a), but this can be improved with more expensive glass materials. For this prototype, the manufacturing company 'HLH prototypes' provided very good plastic primary and secondary reflectors but after some initial testing the secondary's had to be swapped for hand polished aluminium reflectors. This was due to the plastic secondary's melting due to the concentrated light incident on them and hence higher temperatures. The reflectance spectra of the primary and secondary materials were measured and shown in Fig. 5b. The primary plastic mirrors have the advantage of being far lighter than their metallic counterparts and also manufactured accurately using CNC machining with no need for repeated post-polishing that is necessary for CNC'd metal. Depending on the polishing method, the specific curvature of the reflective dish can also be lost. The reflective film used in the CRRH was Reflectech's mirror film (Digrazia and Jorgensen, 2010; ReflecTech.Inc, 2014), this reflective film has a very high reflectance as shown in Fig. 5b and is reliable over many years of UV exposure (Digrazia and Jorgensen, 2010; ReflecTech.Inc, 2014). The operating temperature of this film is however recommended to be a maximum of 60 °C, which would be too low if the film was subject to highly concentrated light. In this system the reflective film is used as part of the CRRH and so should only capture scattered light but experimental testing was carried out to confirm this.

The refractive material used for the homogeniser was Sylguard 184, the transmittance of this was measured for different thicknesses as shown in Fig. 5c and d. As expected the increased thickness of the refractive material reduces the transmittance of the light. For the CRRH, the minimum length the light rays could travel from entrance to exit is 75 mm and the maximum is estimated at ~96 mm (Tang and Wang, 2013). The maximum distance also incurs the maximum no. of reflections within the homogeniser without being reflected back out of the homogeniser entrance aperture (Tang and Wang, 2013). With increased incidence angles and more reflections of the side walls of the homogeniser, more distance will be travelled within the refractive medium and hence more absorption will take place. The first prototype of the CRRH involved careful placement of a reflective film sleeve over the original refractive homogeniser (Fig. 6b and c). This method of manufacturing is not practical and there is no way of ensuring the air gap is maintained without checking by eye. In Fig. 6c, it can be seen where the reflective film is in contact with the refractive material causing a puddle like image midway down the homogeniser side wall and voiding TIR. 3D printing was hence employed to manufacture an outer structure which the reflective film could be adhered to as shown in Fig. 6a. In this way, the air gap thickness could be controlled and sustained.

The 3D printed structures were designed using solidworks to leave a 1 mm gap on the inside between the refractive medium and reflective film. The 3D structure was printed as two halves which were then screwed together as shown in Fig. 6a. The nodes at the top opening of the 3D printed structures are to keep the refractive homogeniser centred. The refractive core of the homogeniser was moulded directly onto the solar cell in 1 step to reduce

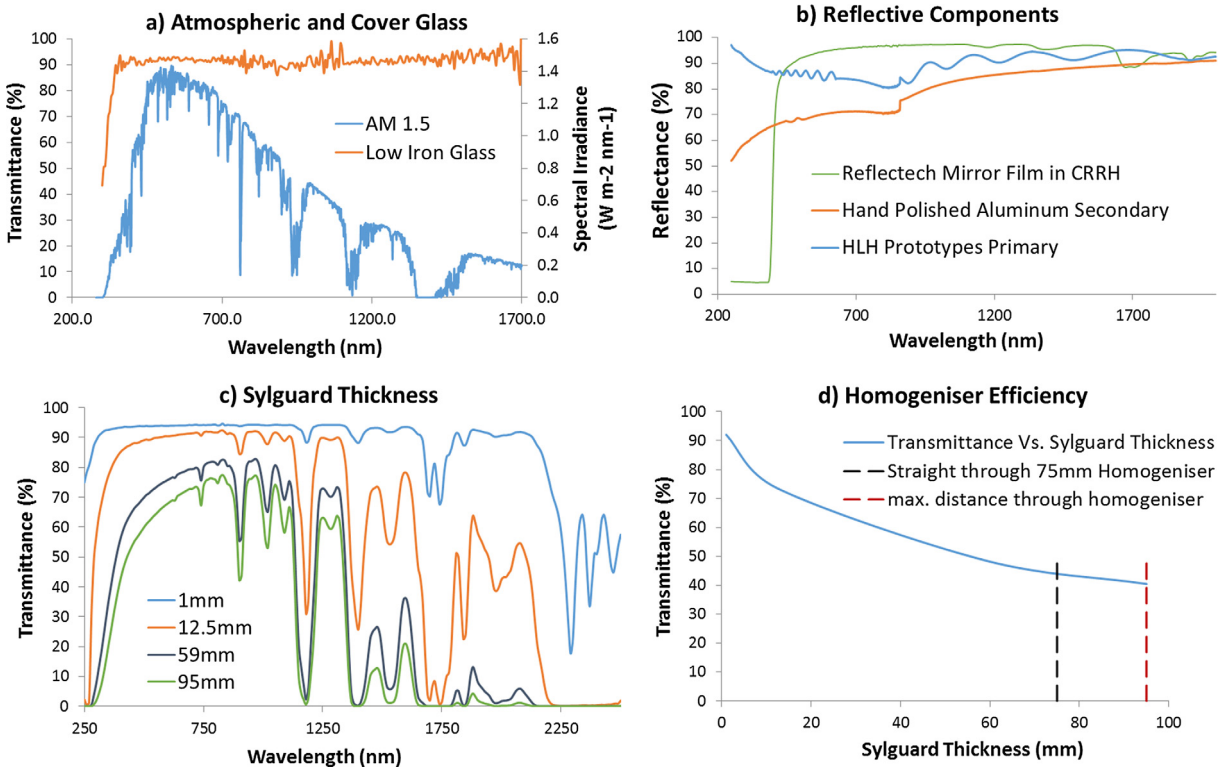

Fig. 5. (a) Cover glass transmittance and atmosphere AM1.5 direct incident irradiance spectrum. (b) Reflectance of the primary and secondary reflector materials. (c) Transmittance spectra for varying thicknesses of sylguard. (d) Transmittance through refractive homogeniser as a function of thickness with estimated minimum and maximum distance the light will travel through the homogeniser. All measurements apart from the AM1.5d were taken with a Perkin Elmer lambda 1050 Spectrophotometer at the University of Exeter, Penryn Campus.

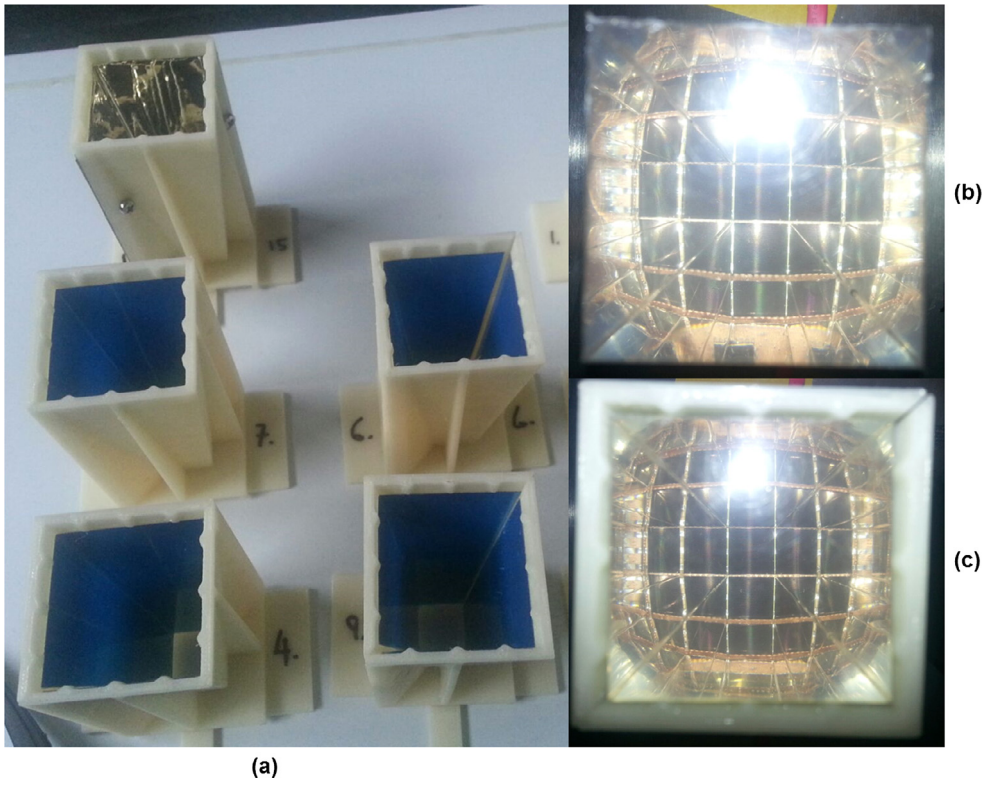

Fig. 6. (a) 3d printed structures with reflective film placed on the inside. A protective blue layer covers the reflective film and is peeled off before use. (b) Standard refractive homogeniser with no reflective film. This is the view from the entry aperture of the homogeniser. (c) Conjugate refractive-reflective homogeniser with 3d structure and reflective film in place. (For interpretation of the references to color in this figure legend, the reader is referred to the web version of this article.)

encapsulate overlap and optical loss, as well as ensuring alignment. This method however also weakens the joint and stability of the homogeniser. When the system is tilted to track the sun during use, the homogeniser may lean to one side and would perhaps stick to the reflective film, voiding TIR or even peeling away from the solar cell itself. These nodes ensure this does not happen and reduce the strain on the joint to the solar cell.

The material used for the 3D printed homogeniser support structure was ABSplus-P430. This is a durable thermoplastic which undergoes heat deflection at 96 °C under 66psi and at 82 °C under 264 psi respectively (Stratasys, 2008). Fig. 6b is a top view of the purely refractive homogeniser and the 1 solar cell reflected in the homogenisers' sides. Due to the reversibility of light paths, the more area seen to be covered by the solar cell and its reflections the more incident light from the sun would reach the solar cell. In this way the improvement can be visually seen when using the CRRH (Fig. 6c) where there is less reflected light and more solar cell coverage. When Fig. 6b and c photos were taken the camera and apparatus was kept in the same place and the only change made was the addition of the reflective sleeve casing (making it CRRH). Visually it can be seen that more light is being absorbed and less reflected back. There is also more solar cell area seen in Fig. 6c near the edges of the refractive medium. This is particularly noticeable at the bottom of Fig. 6c where the reflection of 3 solar cells is seen but at the bottom of Fig. 6b there are only 1 and a half solar cells being reflected. This was confirmed by an increased flux reading from the solar cell.

4. Temperature testing of materials

A complete prototype of the cassegrain set up with the CRRH was subjected to increased temperatures inside a thermal heater to test the ABS plastic of the primary reflector and the CRRH support structure. The full prototype was placed inside a vacuum drying oven (with vacuum mode off) and left for at least 3 h at set temperatures of 60, 70 and 80 °C (not including the time it took for the oven to reach the desired temperature). Higher temperatures were not tested due to the attachment of the solar cell to the CRRH which could be damaged if exposed to higher temperatures. No visual deformation was seen on the CRRH components. When retested under a solar simulator of 1000 W/m^2 there was also no change to the power output after this heat exposure.

The bulk of the homogeniser is made of sylguard which has recommended operational temperature range from −45 °C to 200 °C (Dow Corning Corporation, 2013). The optical transmittance of silicone and encapsulation materials degrades with length of exposer to UV light and excessive heating and cooling (Dow Corning Corporation, 2013; Mcintosh et al., 2009; Miller et al., 2015;

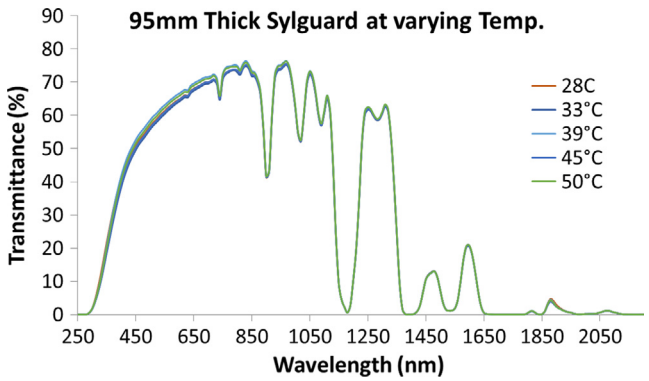

Fig. 7. Transmittance spectra through sylguard at varying temperatures.

Randall Elgin et al., 2007). The transmittance of the sylguard at varying temperatures was measured and the results shown in Fig. 7. There is only a slight difference between these results which is most likely due to soiling and slightly different entrance and exit positions during testing. With curved refractive optics or grooved refractive lenses, the temperature has an effect on the optical properties due to the expansion of the material. In the concentrator tested here the homogeniser has flat refractive surfaces and so the temperature has a negligible effect during operation. It would be expected however that with years of exposure and use, the transmittance quality would decrease.

A 3 by 3 array prototype of the cassegrain concentrator was also built and then tested at the Indian Institute of Technology Madras (IITM) in Chennai as shown in Fig. 8. Under these increased ambient temperatures of around ~30 °C (Nov-Feb), the air temperature inside the 3 by 3 module was measured to be between 50 and 60 °C depending on DNI and duration in sunlight. When the prototype was misaligned with the sun, causing the light to focus on the CRRH 3D printed support structure (Fig. 8a), the plastic material began to melt as shown in Fig. 8b and c. This does not happen when the system is kept aligned within its working range but an improvement to the design would be to fix reflective film or a similar protective layer to shade the 3d printed material from the direct concentrated focusing point. This would ensure the systems components are not at risk of damage if for whatever reason the solar tracker stops working accurately and the system becomes misaligned for >5 min.

As you can see from Fig. 8b, the deformation is localized, confirming that it is only the focal area which is capable of melting the 3d printed plastic. This localization can also be seen in the infrared images shown in Fig. 9. A different plastic cannot be chosen at this time for the 3d printed structure due to the 3d printing process and requirements. Other manufacturing processes could be employed to make the support structure but the accuracy must be within ±0.5 mm. The tapered wall, nodes and feet of the support structure would be difficult to manufacture with a different process and no doubt cost more, especially for small batch prototype orders.

The focal area of the concentrated light was measured to be a far higher temperature than the inside of the module, reaching a maximum of 149 °C with an open (no walls) system and a maximum of 226.3 °C with a closed system (no air ventilation). Thermocouples were used instead of the infrared camera to take all temperature measurements including the focal area temperature as shown in Fig. 9b. The infrared images however also show the overall temperature dispersion within the module and one cassegrain primary was removed to show the difference in temperature when no light concentration takes place (Fig. 9a). From Fig. 9a and b you can see that the temperature of the secondary reflectors, the tops of the homogeniser and the bottom of the

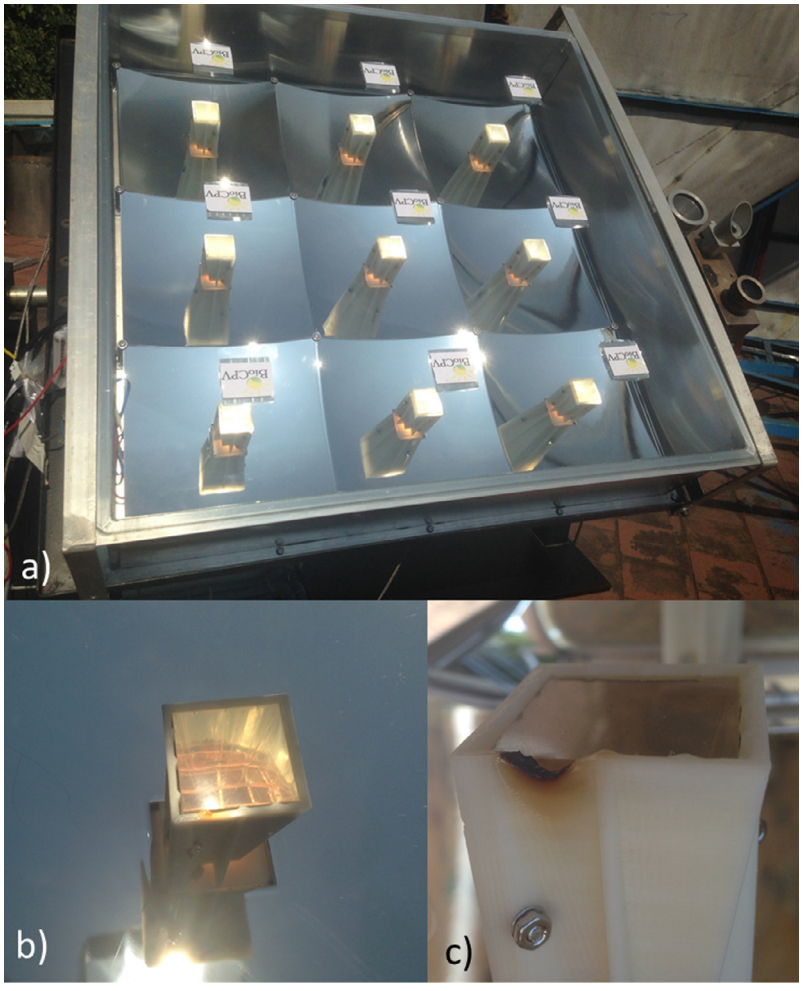

Fig. 8. (a) Photo of complete 3 by 3 prototype with side walls in place (closed) mounted on a 2 axis automatic tracker at IIT Madras, Chennai. (b) Photo of CRRH with concentrated light focusing off-centre onto plastic material of 3d printed support structure and causing burn marks. (c) Close up photo of melting due to >20 min of focused light incident on CRRH plastic support structure.

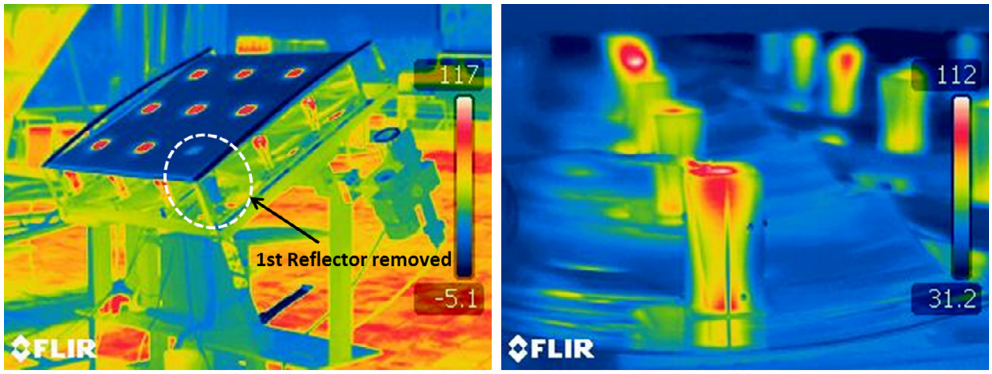

(a) (b)

Fig. 9. (a) Infrared photo of 3 by 3 concentrator prototype with side walls off (open) mounted on solar tracker at IIT Madras, Chennai. The bottom right primary reflector has been removed so there is no concentration of light on the secondary or homogenizer, hence the cooler temperature coloring shown in this corner. (b) Close up of homogenizer situated bottom left of Fig. 8b) with thermocouple used to measure focal area temperature.

homogeniser, near the solar cell, were the higher temperature areas of the system. The high absorption of the homogeniser (Fig. 5c and d) suggests the homogeniser optic to be the most heated part of the system. Prolonged use at these temperatures could damage the sylguard material and transparency over time.

The solar cells themselves were measured using a calibrated K-type thermocouple attached with thermal adhesive to the underside of the cell. Three solar cells were measured, the central, bottom corner and left centre solar cells in the 3 by 3 array. The measured temperatures of the central solar cell varied between 54 and 61 °C for the closed (no air ventilation) system and between 43 and 48 for the open (no walls) system. The left centre cell and corner cell were slightly lower than the central cell temperature but similar to each other and varied between 51 and 57 °C in the closed system. In the open system the middle left and the bottom corner cell temperatures separated more and a temperature of between 40 and 44 °C was measured for the middle left and of 38–40 °C for the bottom corner. These measurements although done with a thermocouple attached to the solar cell assembly are not measuring the direct temperature on the top of the cell which as indicated by the infrared images to be higher. There may be a significant difference even between the top of the solar cell and the bottom of the solar cell due to the concentration of light, insulating homogeniser material and large cooling heat sink on the bottom. As previously suggested, the homogeniser is absorbing most of the thermal radiation but will also be insulating the solar cell. Further detailed thermal analysis would need to be conducted to ensure the operating temperature of the solar cell was not significantly reducing its conversion efficiency. From the difference in temperatures between the open and closed systems, the different cell positions and the rate of heating and cooling of the system it was assumed that the large aluminium heat sink was working effectively at cooling the solar cells, especially with the aid of air movement around the system. The primary reflectors were at a safe lower temperature; hence their bulk plastic material did not melt. With each stage and increase in light concentration, an increase in temperature can also be expected and so 2nd or 3rd stage optics should have a higher working temperature range than the 1st. The location and function of the concentrator system will however have an effect on this.

5. I-V output and incidence angle

The estimated irradiance reaching the solar cell for this prototype is shown in Fig. 10 below. This is resulting from the measured efficiencies of each component being applied to the AM1.5 direct irradiance spectrum (Fig. 5). The low reflectance of the hand polish aluminium secondary reflector over the range ~200–900 nm from Fig. 5 can be seen in Fig. 10 to drop the irradiance over that range down significantly. The main loss however is due to the absorption within the dielectric material used for the CRRH. The transmittance spectra of the homogeniser is shown in Fig. 5c and the average transmittance over 300–1800 nm shown in Fig. 5d. The average transmittance is less than 50% at a thickness of >75 mm. The homogeniser reduces the efficiency significantly in the wavelengths >1100 which the secondary reflector does now. Overall the thick sylgard is the greatest source of loss within the system due to absorption. From Fig. 10 it can be estimated that the optical efficiency is as low as ~35%. Shorter CRRH designs or CRRH optics made of different refractive mediums could have a substantially higher optical efficiency.

The multijunction solar cell used was the 3C42A 10 × 10 mm^2 CPV TJ Solar Cell from Azur Space (Azure Space Solar Power GMBH, 2014). This cell has a wavelength range of ~300–1700 nm and a peak efficiency of 41.5% depending on sun concentration and temperature as shown in Fig. 11.

The solar concentration of the system will be less than 500× which is its ideal geometrical concentration ratio. As can be seen from Fig. 11b, the cell efficiency has a relatively flat relationship with sun concentration at below 500× so the defining parameter for efficiency in this case will be the operating temperature of the solar cell. The temperature of the cell was measured experimentally during operation to vary between 40 and 60 °C which would give a theoretical cell efficiency of ~40.5% but as already suggested a more thorough thermal analysis would be required to know for sure.

The cassegrain concentrator was tested under a continuous type WACOM 1000 W/m^2 class AAA indoor solar simulator (Wacom Electric Company Ltd., 2014) at the university of Exeter Penryn campus with the CRRH and with the standard refractive homogeniser counterpart. I-V traces were taken for a range of alignment angles against the simulated incident light as shown in Fig. 12 below.

The CRRH consistently improved the power output in comparison to the purely refractive homogeniser as shown in Fig. 12. The CRRH increased the Pmax by 3.5% at normal incidence and by 4.5% at 0.5° misalignment. This makes sense as at an increased incidence angle, more light rays should be lost through the side walls of the homogeniser (site 4 in Fig. 4b) and hence the CRRH captures more light and a greater improvement in optical efficiency is seen. At 1° misalignment (the theoretical acceptance

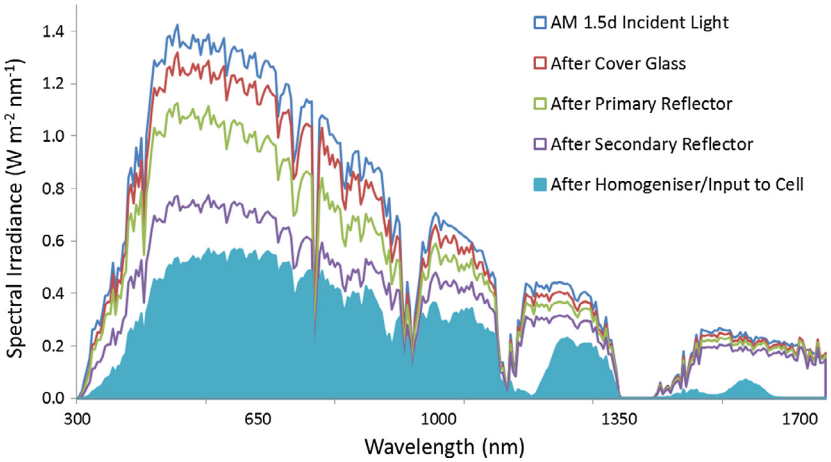

Fig. 10. Graph of irradiance as it filters through the optical stages within the prototype concentrator.

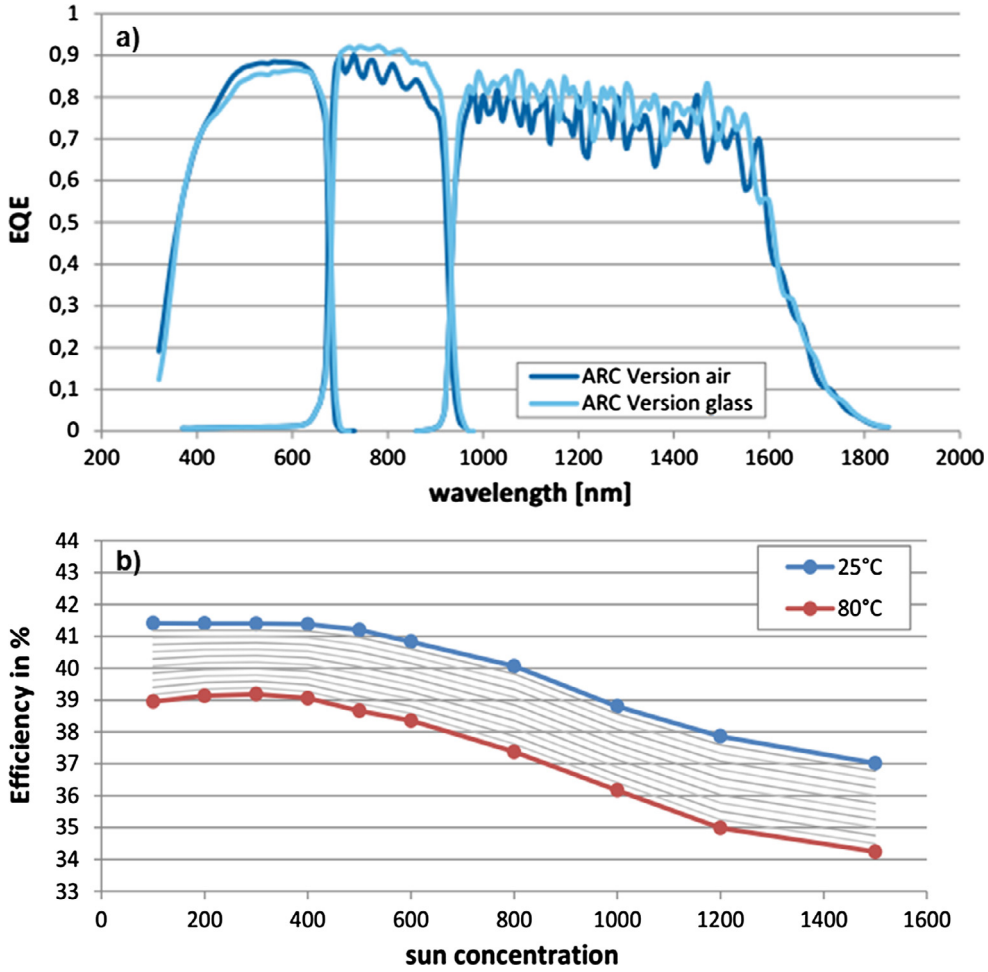

Fig. 11. Graph of conversion efficiency vs. sun concentration for the 10 by 10 mm Azure Space solar cell 3C42 at varying operation temperatures(Azure Space Solar Power GMBH, 2014).

angle of the system), more light is now missing the secondary reflector (site 1 in Fig. 4b) and so the power increases by only 3.7% with the CRRH. At 2 and 3° misalignment the percentage increase in power is 11.3% and 48.7% but this is due to more light being captured at the entrance surface of the CRRH. The CRRH has an entry aperture of 32 mm by 32 mm due to the extra 1 mm air gap added to each side of the original refractive homogeniser of 30 mm by 30 mm entrance aperture. The set-up of the complete cassegrain concentrator is such that light is focused to the centre of the homogenising optic and hence this increased entry aperture effect would only be noticeable when the light began to focus at the edge of the entrance aperture (at 2 or 3° misalignment angles) as shown in Fig. 12b. Any increase in power output is however an advantage. This explains why the power increase of the CRRH in

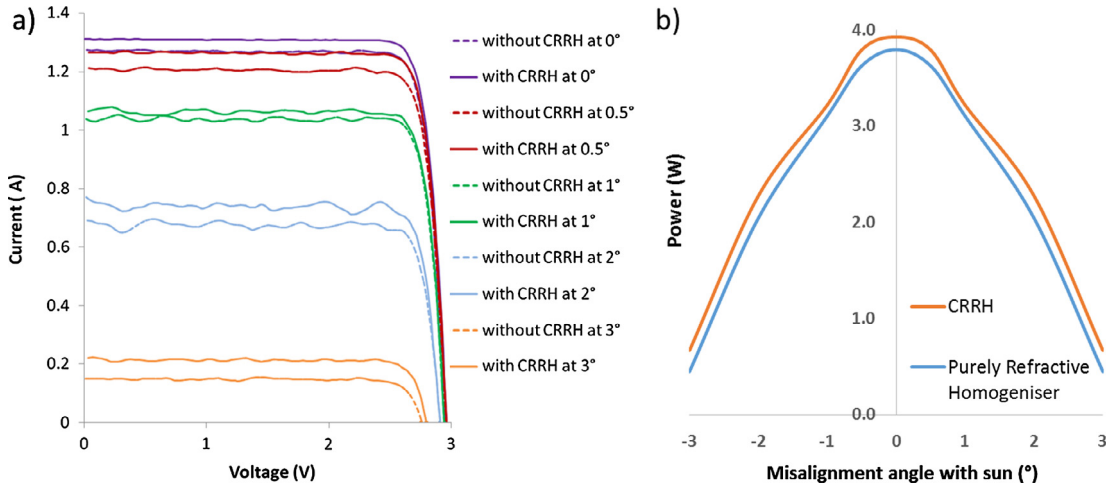

Fig. 12. (a) Comparison of I-V plots for the cassegrain concentrator with a standard refractive homogenizer and with the CRRH at various solar misalignment angles. (b) Power output against full system misalignment angle with normal axis incident light for both homogenizer types.

Fig. 12b stays fairly constant from 2 to 3° despite there being less light incident on the homogeniser optic overall.

The acceptance angle technically does not increase very much from the results shown in Fig. 12b due to the normal incidence power also increasing and hence 90% of that value results in roughly the same acceptance angle as the lower performing pure refractive homogeniser. However, it is clear from Fig. 12a and b that the CRRH outperforms the purely refractive homogeniser. The shape of the CRRH power output in Fig. 12b is slightly unusual but emphasis the stages of loss already discussed in the previous paragraph and in Fig. 4. The optical tolerance of a system is a very important part of a design especially as concentration levels increase for future designs. More complex reflective sleeves consisting of conic curves, grooves or truncated tiling may improve the acceptance angle more significantly. Misalignments in tracker systems are still very common and for high concentration designs can significantly reduce their output from their full potential.

The fill factor for the set up with and without the CRRH was around 0.85 at normal incidence and 0.87 at 1° misalignment and 0.84 at 2–3° misalignment. The absolute efficiency of the system was significantly lower than anticipated due to the low reflection and high absorption of the optics as discussed previously. The temperature of the solar cell could also be reducing the overall efficiency but by how much is not known without a more thorough investigation into the exact temperature of the cell. There are many papers which try to predict the conversion efficiency of solar cells depending on incident irradiance, temperature distribution across the cell, hours of operation and rate of temperature changes during operation.

6. Comparing theoretical predictions to experimental and CAP analysis

The maximum acceptance angle for a 500× geometrical concentration design is 3.59° assuming a refractive index of 1.4 for the homogeniser. The maximum acceptance angle is never attainable due to a variety of non-ideal contributors such as manufacturing errors, temperature effects and material properties. The concentration-acceptance product (CAP) does however give a value of how good the design is in comparison to its theoretical limits. The higher the CAP the more fulfilling the design is for that specific geometric concentration level. A summary table of the optical efficiency, resulting concentration ratio, acceptance angle and the associated CAP is given below (see Table 1).

For this system, the CAP is roughly a third of its ideal if we only look at the optimised design detailed in the previous theoretical studies. This is relatively standard in comparison to other designs of similar concentration ratios. The addition of the CRRH instead of a purely refractive homogeniser slightly increases the CAP. Once the realistic optical efficiency is introduced the CAP falls significantly, especially due to the high absorption of the homogeniser as shown in Fig. 5. Using a different material such as Glass or PMMA should reduce the absorption and improve the performance significantly.

The maximum theoretical optical efficiency increase due to the CRRH was 7.76% in the simulations carried out previously by Shanks et al. (2016a). Experimental measurements with a Fresnel lens set up produced 6.7% but it was suspected that some light entered the air gap in this experiment at normal incidence due to the slightly larger focal area using the Fresnel lens. The maximum experimental increase in power measured from these studies was 4.5% using the cassegrain set up which had a tighter focal spot incident only on the refractive core of the CRRH. The simulated optical efficiency from before assumed a lower absorption for the homogeniser refractive material. In this study sylgard 184 was utilised and had significant absorption losses as shown in Figs. 5c and d and 10, especially in the infrared range. This results in overall a lower optical efficiency of the system and a lower concentration incident on the cell than theoretically suggested. The benefit of the CRRH is expected to increase with concentration ratio as there is more light for it to recapture.

The absorption losses are more significant in the infrared range and in theory these wavelengths would benefit most from the CRRH due to their slightly higher critical angle requirements. This slight increase in critical angle (+0.5° between 589 nm and 1554 nm) as wavelength size increases may or may not be negligible depending on how close to the critical angle the light rays are originally. It is well known that temperature can alter the refractive index and shape of a dielectric optic which in turn can push an optimised design over or under its peak performance parameters. The same could be occurring to some degree in this design as there are such high temperatures present on the homogeniser in particular. A fully optimised homogeniser would just fulfil TIR conditions and no more, achieving the maximum concentration ratio and acceptance angle before optical efficiency decreased too low. In which case anything that could risk changes to the refractive index, angle of incidence or shape of the optic would again alter the optics performance and optical efficiency.

Table 1
Cap analysis of cassegrain concentrator for different optical efficiencies.

Design scenario	Optical efficiency	Effective concentration ratio	Acceptance angle (°)	CAP
Ideal (maximum values possible)	100%	500×	3.59	1.4 (n)
Geometric design (no reflection or absorption losses) (Shanks et al., 2016b)	100%	500×	1.2	0.468
Standard (not conjugate) Refractive Homogeniser (theoretical losses) (Shanks et al., 2016a)	68%	340×	1	0.322
CRRH (theoretical losses) (Shanks et al., 2016a)	71%	355×	1	0.329
CRRH (measured)	~40%	200×	~0.8	0.197

The simulations carried out for this design also did not take into account the conversion efficiency of the solar cell or temperature effects. All of the above contribute to the difference between the theoretical and experimental results. From this study a 4.5% increase in power output is the maximum realistic benefit of the CCRH within a cassegrain concentrator set up of similar concentration and manufactured with similar materials and methods.

7. Discussion and future outlook

The CRRH optic is a simple but effective method to improve the power output of a concentrator system utilising a receiver/homogenising optic. How much the CRRH will benefit the system depends on the input energy to the homogenizer (whether this be due to a higher concentration ratio or optical efficiency of the system) and the manufacturing quality of the homogenising optic. High accuracy manufacturing with very smooth surface finishes for the purely refractive homogenizer should see minimal improvement with the addition of a reflective sleeve to make the CRRH. In this study, the refractive homogenizer was manufactured using sylgard material and a mould made of polished aluminium which is a common method for small optics such as this.

The theoretical analysis suggested a possible increase in power output of 7.76% and the experimental testing carried out in this study gave a maximum of 4.5% power increase. The difference in these values is most likely due to high absorption by the thick homogenizer and possibly the high operating temperature of the solar cell. Small misalignments within the system; and the lower reflectance of the primary and secondary reflectors also reduces the amount of light available to recover if scattered. As previously discussed other effects such as temperature and refractive index change could be altering the optical efficiency and acceptance angle of the homogenizer. It is suggested for future work in high and ultrahigh concentration levels to not only design for manufacturing tolerances but also temperature tolerances. This may mean choosing design variables which actually precede the optimum performance design at room temperature but will continue to fulfill TIR or similar parameter conditions at high operating temperatures where the refractive index has decreased. From this and previous analysis of the CRRH (Shanks et al., 2016a), it would seem the CRRH's benefit to optical efficiency increases with an increase in input light, such as for higher concentration ratio designs. This also makes sense as higher concentration systems are also more prone to diverging focal spots and a wider range of light ray angles incident on the secondary and tertiary optics. It can also be deduced from these experimental results that roughly 40% of a simulated performance increase, due to the CRRH or a similar conjugate refractive reflective optic in comparison to a purely refractive counterpart, can be realized in experimental testing.

The structure of the CRRH could be improved by using a different material for the support structure such as aluminium or similar which can handle the very high temperatures of the focused light. This type of structure however may be heavy depending on the design. A skeletal support structure may not be strong enough to hold the reflective film in place. Sheets of polished aluminium could be used to surround the refractive medium but manufacturing would have to be accurate to ensure the ~1 mm air gap between the two materials. Some kind of node seems to be beneficial to maintain alignment. Perhaps the refractive homogenizer and its matching reflective casing could be manufactured together and then separated slightly. A simple solution to avoid the 3D printed structures melting in this study would be to add a protective layer to the top edge of the CRRH plastic material to diffusely reflect the focused light safely away. Improving the alignment and focusing capabilities of the system would also reduce the risk of the focused light hitting the 3D printed plastic structure. Another improvement would be to have a refractive medium with a higher transmittance or to perhaps try a lens walled approach to reduce absorption losses through the thick homogenizer. Overall this concept of conjugate refractive reflective optics should be researched further for other shapes and their benefit analyzed.

The use of plastic core optics appears to be a valuable option, especially for the prototyping stage of CPV. From these results they are however limited to low concentration optics, primary optics in higher concentration set ups or as support structures not subject to focused light. Their durability with time should however be tested further.

8. Conclusion

The Conjugate Refractive Reflective Homogeniser has been experimentally tested within a 500× geometric concentration cassegrain design. A prototype of the complete system was built and experimentally tested. Measurements showed a 4.5% increase in power. This was ~40% of the theoretical improvement calculated by simulations (7.76%). Temperature testing was also carried out on the components and the 3D printed support structure for the CRRH was found to be inadequate at coping with the direct focused sunlight. However, the resulting deformation in the structure only occurs when there is a misalignment of 2–3° in the system. The high operating temperature should not affect the transmittance of the homogenizer since flat refractive surfaces are used and hence expansion of the refractive medium should not alter the direction of light. Improving the design by using a protective layer on the 3d printed support structure should easily solve this issue. The experimental tests confirmed the CRRH can improve the power output of a cassegrain concentrator of this design and 500× geometric concentration ratio.

Acknowledgments

This work was partly funded by the Newton Bhabha PhD Placement fund and partly by DST, India (Ref No: DST/SEED/INDO-UK/002/2011) and EPSRC, UK, (Ref No: EP/J000345/1) through the BioCPV project. Authors acknowledge all funding agencies for the support. In support of open access research all underlying article materials (such as data, samples or models) can be accessed upon request via email to the corresponding author.

References

Azure Space Solar Power GMBH, 2014. Enhanced Fresnel Assembly - EFA Type: 3C42A – with $10 \times 10\ mm^2$ CPV TJ Solar Cell Application: Concentrating Photovoltaic (CPV) Modules.

Baig, H., 2015. Enhancing Performance of Building Integrated Concentrating Photovoltaic Systems (Article). University of Exeter.

Baig, H., Heasman, K.C., Mallick, T.K., 2012. Non-uniform illumination in concentrating solar cells. Renew. Sustain. Energy Rev. 16, 5890–5909. http://dx.doi.org/10.1016/j.rser.2012.06.020.

Baig, H., Sarmah, N., Chemisana, D., Rosell, J., Mallick, T.K., 2014. Enhancing performance of a linear dielectric based concentrating photovoltaic system using a reflective film along the edge. Energy 73, 177–191.

Baig, H., Sellami, N., Mallick, T.K., 2015. Trapping light escaping from the edges of the optical element in a concentrating photovoltaic system. Energy Convers. Manage. 90, 238–246. http://dx.doi.org/10.1016/j.enconman.2014.11.026.

Benítez, P., Miñano, J.C., Zamora, P., Mohedano, R., Cvetkovic, A., Buljan, M., Chaves, J., Hernández, M., 2010. High performance Fresnel-based photovoltaic concentrator. Opt. Exp. 18, A25–A40. http://dx.doi.org/10.1364/OE.18.000A25.

Canavarro, D., Chaves, J., Collares-Pereira, M., 2013. New second-stage concentrators (XX SMS) for parabolic primaries; comparison with conventional parabolic trough concentrators. Sol. Energy 92, 98–105. http://dx.doi.org/10.1016/j.solener.2013.02.011.

Chen, Y.T., Ho, T.H., 2013. Design method of non-imaging secondary (NIS) for CPV usage. Sol. Energy 93, 32–42. http://dx.doi.org/10.1016/j.solener.2013.03.013.

Chong, K.K., Lau, S.L., Yew, T.K., Tan, P.C.L., 2013. Design and development in optics of concentrator photovoltaic system. Renew. Sustain. Energy Rev. http://dx.doi.org/10.1016/j.rser.2012.11.005.

Digrazia, M., Jorgensen, G., 2010. Reflectech Mirror Film: Design Flexibility and Durability in Reflecting Solar Applications.

Dow Corning Corporation, 2013. Electronics Sylgard ® 184 Silicone Elastomer. http://dx.doi.org/10.1017/CBO9781107415324.004.

Dreger, M., Wiesenfarth, M., Kisser, A., Schmid, T., Bett, A.W., 2014. Development and Investigation of A CPV Module with Cassegrain Mirror Optics, in: CPV-10.

Fend, T., Hoffschmidt, B., Jorgensen, G., Kuster, H., Kruger, D., Pitz-Paal, R., Rietbrock, P., Riffelmann, K.J., 2003. Comparative assessment of solar concentrator materials. Sol. Energy 74, 149–155. http://dx.doi.org/10.1016/S0038-092X(03)00116-6.

Fraas, L.M., 2014. Low-Cost Solar Electric Power. Springer International Publishing, Cham. http://dx.doi.org/10.1007/978-3-319-07530-3.

Gordon, J.M., Feuermann, D., Young, P., 2008. Unfolded aplanats for high-concentration photovoltaics. Opt. Lett. 33, 1114–1116.

Hatwaambo, S., Hakansson, H., Nilsson, J., Karlsson, B., 2008. Angular characterization of low concentrating PV–CPC using low-cost reflectors. Sol. Energy Mater. Sol. Cells 92, 1347–1351. http://dx.doi.org/10.1016/j.solmat.2008.05.008.

Kaushika, N., Reddy, K., 2000. Performance of a low cost solar paraboloidal dish steam generating system. Energy Convers. Manage. 41, 713–726. http://dx.doi.org/10.1016/S0196-8904(99)00133-8.

Leutz, R., Suzuki, A., 2001. Nonimaging Fresnel Lenses: Design and Performance of Solar Concentrators. Springer Science & Business Media.

McDonald, M., Horne, S., Conley, G., 2007. Concentrator Design to Minimize LCOE 6649, 66490B-66490B-11. http://dx.doi.org/10.1117/12.735738.

Mcintosh, K.R., Cotsell, J.N., Cumpston, J.S., Norris, A.W., Powell, N.E., Ketola, B.M., 2009. The Effect of Accelerated Aging Tests on the Optical Properties of Silicone and EVA Encapuslants.

Miller, D.C., Annigoni, E., Ballion, A., Bokria, J.G., Bruckman, L.S., Burns, D.M., Chen, X., Elliott, L., Feng, J., French, R.H., Fowler, S., Gu, X., Hacke, P.L., Honeker, C.C., Kempe, M.D., Khonkar, H., Köhl, M., Perret-Aebi, L.-E., Phillips, N.H., Scott, K.P., Sculati-Meillaud, F., Shioda, T., Suga, S., Watanabe, S., Wohlgemuth, J.H., 2015. Degradation in PV encapsulation transmittance: an interlaboratory study towards a climate-specific test preprint degradation in PV encapsulation transmittance: an interlaboratory study towards a climate-specific test. In: 42nd IEEE Photovoltaic Specialists Conference, New Orleans, Louisiana.

Randall Elgin, Bill Riegler, Rob Thomaier, 2007. How Temperature Effects Transmission of Silicone Encapsulants a Survey of the effects of temperature in optically clear silicones. Photonics Spectra.

ReflecTech.Inc, 2014. ReflecTech Mirror Film Technical [WWW Document]. URL <http://www.reflectechsolar.com/technical.html> (accessed 4.20.16).

Roman, R.J., Peterson, J.E., Goswami, D.Y., 1995. An off-axis cassegrain optimal design for short focal length parabolic solar concentrators. J. Sol. Energy Eng. 117, 51. http://dx.doi.org/10.1115/1.2847742.

Shanks, K., Baig, H., Senthilarasu, S., Reddy, K.S., Mallick, T.K., 2016a. Conjugate refractive–reflective homogeniser in a 500× Cassegrain concentrator: design and limits. IET Renew. Power Gener. 1–8. http://dx.doi.org/10.1049/iet-rpg.2015.0371.

Shanks, K., Sarmah, N., Ferrer-Rodriguez, J.P., Senthilarasu, S., Reddy, K.S., Fernández, E.F., Mallick, T., 2016b. Theoretical investigation considering manufacturing errors of a high concentrating photovoltaic of cassegrain design and its experimental validation. Sol. Energy 131, 235–245. http://dx.doi.org/10.1016/j.solener.2016.02.050.

Shanks, K., Senthilarasu, S., Mallick, T.K., 2016c. Optics for concentrating photovoltaics: trends, limits and opportunities for materials and design. Renew. Sustain. Energy Rev. 60, 394–407.

Shanks, K., Senthilarasu, S., Mallick, T.K., 2015. High-concentration optics for photovoltaic applications. In: Pérez-Higueras, P., Fernández, E.F. (Eds.), High Concentrator Photovoltaics: Fundamentals, Engineering and Power Plants, Green Energy and Technology.. Springer International Publishing, Cham, pp. 85–113. http://dx.doi.org/10.1007/978-3-319-15039-0.

Stratasys, 2008. ABSplus Properties.

Tang, R., Wang, J., 2013. A note on multiple reflections of radiation within CPCs and its effect on calculations of energy collection. Renew. Energy 57, 490–496. http://dx.doi.org/10.1016/j.renene.2013.02.010.

Terry, C.K., Peterson, J.E., Goswami, D.Y., 2012. Terrestrial solar-pumped iodine gas laser with minimum threshold concentration requirements. J. Thermophys. Heat Transf.

Terry, C.K., Peterson, J.E., Goswami, D.Y., 1996. Feasibility of an iodine gas laser pumped by concentrated terrestrial solar radiation. J. Sol. Energy Eng. 118, 136. http://dx.doi.org/10.1115/1.2848006.

Tsai, C.-Y., 2013. Enhanced irradiance distribution on solar cell using optimized variable-focus-parabolic concentrator. Opt. Commun. 305, 221–227. http://dx.doi.org/10.1016/j.optcom.2013.04.052.

Victoria, M., Domínguez, C., Antón, I., Sala, G., 2009. Comparative analysis of different secondary optical elements for aspheric primary lenses. Opt. Exp. 17, 6487–6492.

Victoria, M., Dominguez, C., Askins, S., Anton, I., Sala, G., 2013. Experimental analysis of a photovoltaic concentrator based on a single reflective stage immersed in an optical fluid. Prog. Photovoltaics Res. Appl. http://dx.doi.org/10.1002/pip.2381.

Wacom Electric Company Ltd., 2014. Wacom Product Solar Simulator [WWW Document]. URL <http://www.wacom-ele.co.jp/en/products/solar/normal/> (accessed 11.14.16).

Winston, R., 1970. Light collection within the framework of geometrical optics. J. Opt. Soc. Am. 60, 245. http://dx.doi.org/10.1364/JOSA.60.000245.

Xu, Y.J., Liao, J.X., Cai, Q.W., Yang, X.X., 2013. Preparation of a highly-reflective TiO_2/SiO_2/Ag thin film with self-cleaning properties by magnetron sputtering for solar front reflectors. Sol. Energy Mater. Sol. Cells 113, 7–12. http://dx.doi.org/10.1016/j.solmat.2013.01.034.

Yehezkel, N., Appelbaum, J., Yogev, a., Oron, M., 1993. Losses in a three-dimensional compound parabolic concentrator as a second stage of a solar concentrator. Sol. Energy 51, 45–51. http://dx.doi.org/10.1016/0038-092X(93)90041-L.

Yin, L., Huang, H., 2008. Brittle materials in nano-abrasive fabrication of optical mirror-surfaces. Precis. Eng. 32, 336–341. http://dx.doi.org/10.1016/j.precisioneng.2007.09.001.